Multi-Scale Multi-Target Domain Adaptation for Angle Closure Classification

Zhen Qiu[1,5], Yifan Zhang[2], Fei Li[3], Xiulan Zhang[3],
Yanwu Xu[4], and Mingkui Tan[1,6*]

[1]South China University of Technology, [2]National University of Singapore,
[3]Sun Yat-sen University, [4]Baidu Inc., [5]Pazhou Laboratory,
[6]Key Laboratory of Big Data and Intelligent Robot, Ministry of Education

Abstract. Deep learning (DL) has made significant progress in angle closure classification with anterior segment optical coherence tomography (AS-OCT) images. These AS-OCT images are often acquired by different imaging devices/conditions, which results in a vast change of underlying data distributions (called "data domains"). Moreover, due to practical labeling difficulties, some domains (*e.g.,* devices) may not have any data labels. As a result, deep models trained on one specific domain (*e.g.,* a specific device) are difficult to adapt to and thus may perform poorly on other domains (*e.g.,* other devices). To address this issue, we present a multi-target domain adaptation paradigm to transfer a model trained on one labeled source domain to multiple unlabeled target domains. Specifically, we propose a novel Multi-scale Multi-target Domain Adversarial Network (M2DAN) for angle closure classification. M2DAN conducts multi-domain adversarial learning for extracting domain-invariant features and develops a multi-scale module for capturing local and global information of AS-OCT images. Based on these domain-invariant features at different scales, the deep model trained on the source domain is able to classify angle closure on multiple target domains even without any annotations in these domains. Extensive experiments on a real-world AS-OCT dataset demonstrate the effectiveness of the proposed method.

Keywords: Angle Closure Classification · Unsupervised Multi-target Domain Adaptation · Anterior Segment Optical Coherence Tomography.

1 Introduction

Glaucoma is the foremost cause of irreversible blindness [28,31]. Since the vision loss is irreversible, early detection and precise diagnosis for glaucoma are essential to vision preservation. A common type of glaucoma is angle closure, where the anterior chamber angle (ACA) is narrow as shown in Fig. 1(b). Such an issue leads to blockage of drainage channels that results in pressure on the optic nerve [7]. To identify this, anterior segment optical coherence tomography (AS-OCT) has been shown an effective approach for the evaluation of the ACA structure [15] and is thus widely used for angle closure classification [12,13].

---

* Corresponding author.

(a) AS-I (open angle)   (b) AS-I (narrow angle)

(c) AS-II   (d) AS-III
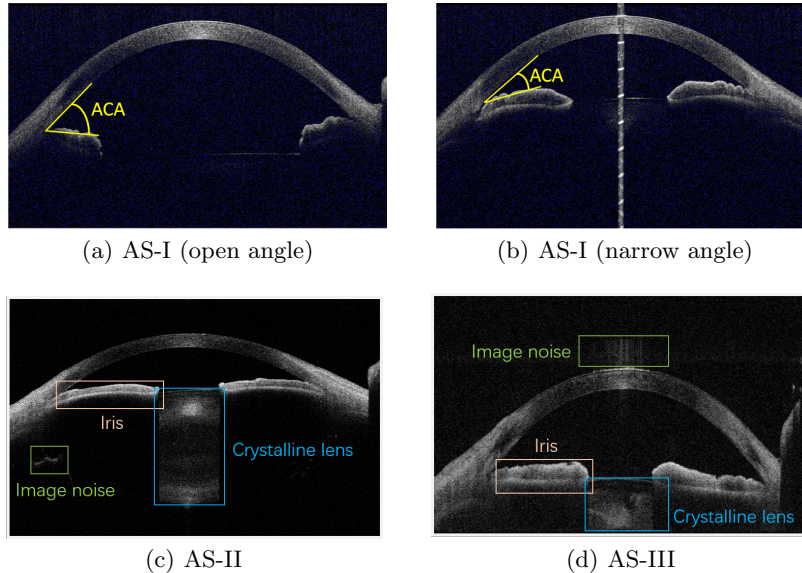
Fig. 1. Illustration of different types of anterior chamber angle (ACA) and different data domains. Specifically, ACA consists of two categories: open angle (a) and narrow angle (b). In addition, different imaging devices/techniques may result in different data domains of anterior segment (AS) images, *e.g.,* AS-I (a-b), AS-II (c) and AS-III (d), which differ in terms of the crystalline lens [4], image noises [1], and image resolutions.

Despite the success of deep learning in computer-aided diagnosis, it hinges on massive annotated images for training [18]. Thanks to AS-OCT devices and hence a growing number of labeled AS-OCT data for deep model training, remarkable performance has been achieved on angle closure classification [5,23]. However, different imaging devices/conditions intrinsically lead to a vast change of underlying data distributions [38], which means that the AS-OCT images may come from different "domains". As a result, deep models trained on one domain (*e.g.,* a specific device) can hardly generalize to other domains [22] (*e.g.,* other devices). More critically, it is impractical to customize deep models for each domain, since annotation costs for such specific-customized images are inevitably expensive. Note that due to labeling difficulties, we may not have any labeled data for some domains.

To solve this issue, one may explore unsupervised domain adaptation [2,10,19,27,32,33,34,41], which leverages the labeled data on a source domain to improve the performance on an unlabeled target domain. Most existing methods [3,38,40,29,16] focus on pair-wise adaptation from one source domain to one target domain. However, in angle closure classification tasks, AS-OCT images are often acquired via diverse imaging devices (*e.g.,* CASIA-I or CASIA-II), imaging conditions (*e.g.,* light or dark environment) and preprocessing techniques. In other words, doctors need to classify AS-OCT images from different domains. Therefore, it is more practical to study multi-target domain adaptation [11,26,36] for angle closure classification.
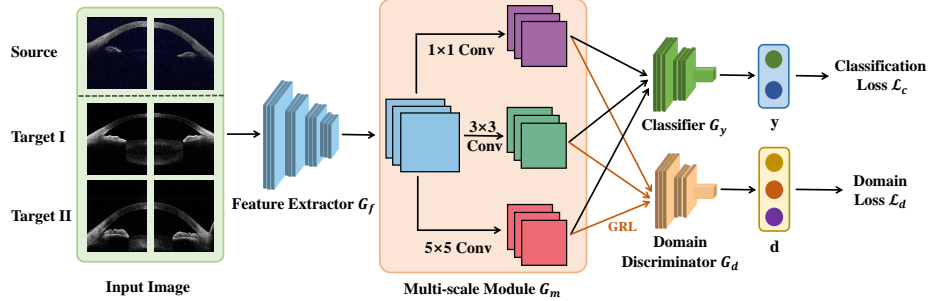
To be specific, multi-target domain adaptation aims to leverage the annotations on one source domain to improve the performance of multiple unlabeled target domains. Despite the importance, it remains largely unexplored for medical images analysis, especially in angle closure classification.

Multi-target domain adaptation with AS-OCT image poses two challenges. The first challenge is the domain discrepancies among multiple domains, which results from different imaging devices, imaging conditions, and preprocessing techniques. As shown in Fig. 1, the AS-OCT images from different domains may differ in terms of the crystalline lens [4], image noises [1] and image resolutions. As a result, directly applying the model trained on the source domain tends to perform poorly on the multi-target domains. The second challenge is how to capture both local and global information of AS-OCT images for angle closure classification. In practice, ophthalmologists classify angle closure based on both local information (*e.g.,* anterior chamber angle (ACA) and iris curvature) and global information (*e.g.,* anterior chamber width and cornea structure) [6]. However, most deep neural networks (DNNs) tend to learn global features without paying attention to fine-grained information of the images, *e.g.,* ACA in AS-OCT images. Since the measurement of small regions (*e.g.,* trabecular iris angle and angle opening distance [6]) in ACA is highly important for this task, it is difficult for existing DNN models to effectively classify angle closure. As a result, most existing DNN-based unsupervised domain adaptation methods may fail to handle such a challenging task.

To handle the two challenges, we explore multi-domain adversarial learning and multi-scale feature extraction for angle closure classification. Specifically, to alleviate the domain discrepancies, we resort to domain adversarial learning, which is one of the mainstream paradigms for pair-wise unsupervised domain adaptation [38,40]. Meanwhile, since there exists low contrast and vast noise in local regions of AS-OCT images (*e.g.,* trabecular iris angle and angle opening distance [6]), capturing fine-grained information with a fixed scale of neural filter is intractable. Therefore, we propose to explore multi-scale convolutional filters for promoting fine-grained representation extraction [7,37]. Following these ideas, we present a novel Multi-scale Multi-target Domain Adversarial Network (M2DAN). In M2DAN, a new multi-scale module is developed to capture global and local information of AS-OCT images. Such a module consists of three convolutional branches with different filter sizes, which are used to extract multi-scale features. Meanwhile, M2DAN conducts multi-domain adversarial learning for each convolutional branch separately, so that it can learn domain-invariant features at different scales. Based on the extracted multi-scale domain-invariant features, the classifier trained on the source domain is able to conduct angle closure classification effectively on the multiple target domains.

We summarize the main contributions of this paper as follows:

- We propose a novel Multi-scale Multi-target Domain Adversarial Network for angle closure classification. By exploring a new multi-scale scheme and multi-domain adversarial learning, the proposed method is able to learn multi-scale domain-invariant features and effectively classify the angle closure.

Fig. 2. The scheme of Multi-scale Multi-target Domain Adversarial Network. Specifically, the multi-scale module consists of three convolutional branches with different filter sizes. Then, we use a shared domain discriminator to distinguish features from each branch separately for scale-aware domain adaptation, while we concatenate all features for classification. We implement domain adversarial training through Gradient Reverse Layer (GRL) [8].

– To the best of our knowledge, our work is the first to study multi-target domain adaptation for angle closure classification, which enhances the applications of deep learning in early detection and precise diagnosis for angle closure glaucoma.
– Extensive experiments demonstrate the effectiveness and superiority of the proposed method on a real-world anterior segment optical coherence tomography dataset with three domains.

2   Method

2.1   Problem Definition

We consider two practical challenges in AS-OCT based angle closure classification task: 1) the distribution changes of different domains (*e.g.,* devices); 2) the lack of labeled data for multiple domains. We tackle them by adapting a model learned on a source domain to B target domains. In total we consider $(B+1)$ domains. For convenience, we introduce a domain label vector $\mathbf{d}_i \in \{0,1\}^{B+1}$ to indicate the domain labels of each sample. Then, let $\mathcal{D}_s = \{\mathbf{x}_i, \mathbf{y}_i, \mathbf{d}_i\}_{i=1}^{n_s}$ be the source domain data and $\mathcal{D}_t = \{\mathbf{x}_j, \mathbf{d}_j\}_{j=1}^{n_t}$ be the unlabeled data collected from B target domains, where $\mathbf{y}_i$ denotes the class label of source domain data, and n_s and n_t denote the numbers of samples in $\mathcal{D}_s$ and $\mathcal{D}_t$, respectively.

Note that given a specific task, all domains share the same label space, but only the source domain data are labeled. The primary goal of this paper is to learn a well-performed deep neural network for multiple target domains, using both labeled source samples and unlabeled target samples. Unfortunately, since we have no labeled target data, how to conduct effective domain adaptation to multiple target domains is very challenging.

2.2   Multi-scale Multi-target Domain Adversarial Network

To enforce effective domain adaptation from the source domain $\mathcal{D}_s$ to the multiple target domain $\mathcal{D}_t$, we address the challenges from two aspects: (1) we seek to alleviate the domain discrepancies among multiple domains with domain adversarial learning; (2) Note that beyond the distribution changes, the $B+1$ domains also share some intrinsic properties as they are dealing with the same task, *e.g.,* angle closure classification. We thus exploit both local and global information of AS-OCT images for angle closure classification with a multi-scale scheme. Given the above motivations, we propose a multi-scale multi-target domain adversarial network (M2DAN). As shown in Fig. 2, M2DAN consists of four components: a feature extractor G_f and a multi-scale module G_m, a classifier G_y for task prediction, and a domain discriminator G_d to discriminate multi-scale features of images from different domains. To be specific, the multi-scale module G_m is developed to extract features with multi-scale information.

In the angle closure classification, both local information (*e.g.,* iris curvature and angle opening distance) and global information (*e.g.,* cornea structure [7]) plays important roles. The local information can be used to obtain several major clinical measurements for clinical diagnosis [24], while the global cornea structure offers various cues associated with risk factors for angle-closure glaucoma [7]. To capture them, the multi-scale module consists of three parallel convolutional branches with different filter sizes (*i.e.,* 1×1, 3×3 and 5×5) to extract features from different scales. Here, all feature maps have the same spatial size through padding. We then send the feature maps at different scales into the domain discriminator separately for multiple domain adaptation, while we concatenate all these features for classification. In this way, we are able to extract domain-invariant features with multi-scale information, which helps the classifier to make more accurate predictions on the target domains.

To train M2DAN, we employ the following two strategies. First, inspired by most domain adaptation methods [3,38,26], we adopt domain adversarial learning to enforce the multi-scale feature extractor $G_m \circ G_f$ to capture multi-scale domain-invariant features, so that the discrepancy among multiple domains is minimized. To be specific, a shared domain discriminator G_d is trained to adequately distinguish features of images from different domains by minimizing a domain loss $\mathcal{L}_d$. Meanwhile, $G_m \circ G_f$ is trained to confuse the domain discriminator by maximizing $\mathcal{L}_d$. Note that, domain adversarial learning is applied to each branch of the multi-scale module separately for learning multi-scale domain-invariant features. Second, we train the backbone network (G_f, G_m, G_y) via a classification loss $\mathcal{L}_c$ to make it imbalance-aware and discriminative. The overall training of M2DAN is to solve the following problem:

$$\min_{\theta_f, \theta_m, \theta_y} \max_{\theta_d} \underbrace{-\alpha \mathcal{L}_d(\theta_f, \theta_m, \theta_d)}_{\text{domain loss}} + \underbrace{\lambda \mathcal{L}_c(\theta_f, \theta_m, \theta_y)}_{\text{classification loss}} \qquad (1)$$

where $\theta_f, \theta_m, \theta_y, \theta_d$ indicate the parameters of G_f, G_m, G_y and G_d, respectively. Moreover, α and λ denote the trade-off parameters for different losses. In next sections, we will detail the domain loss $\mathcal{L}_d$ and the classification loss $\mathcal{L}_c$.

2.3   Domain Loss for Multi-target Domain Adaptation

Diverse imaging devices and techniques intrinsically result in discrepancies among image domains. In practice, doctors often need to classify angle closure based on AS-OCT images from multiple target domains. However, existing unsupervised domain adaptation for medical images mainly focuses on two domains and cannot handle this practical problem.

To solve this, inspired by multi-class classification via cross-entropy, we conduct multi-target domain adaptation via a multi-domain loss as follows:

$$\mathcal{L}_d(\theta_f, \theta_m, \theta_d) = -\frac{1}{n} \sum_{i=1}^{n} \mathbf{d}_i^\top \log(\hat{\mathbf{d}}_i), \tag{2}$$

where $\hat{\mathbf{d}}_i = G_d(G_m(G_f(\mathbf{x}_i)))$ denotes the prediction of the domain discriminator $w.r.t.$ $\mathbf{x}_i$, and n denotes the overall number of data. Moreover, since different branches in the multi-scale module share the same domain discriminator, we use the same domain loss for them without explicitly mentioning branches. In this way, M2DAN is able to capture domain-invariant features at different scales.

2.4   Classification Loss for Angle Closure Classification

For the task of angle closure classification, we can adopt any classification losses to train the network, $e.g.,$ cross-entropy. Nevertheless, since the class-imbalanced issue commonly exist in this task, we use the focal loss [17] as follows:

$$\mathcal{L}_{fo}(\theta_f, \theta_m, \theta_y) = -\frac{1}{n_s} \sum_{i=1}^{n_s} \mathbf{y}_i^\top \big((1 - \hat{\mathbf{y}}_i)^\gamma \odot \log(\hat{\mathbf{y}}_i)\big), \tag{3}$$

where $\hat{\mathbf{y}}_i = G_y(G_m(G_f(\mathbf{x}_i))$ denotes the prediction of the classifier $w.r.t.$ $\mathbf{x}_i$, and n_s denotes the number of **labeled source samples**. Moreover, $\odot$ denotes the element-wise product and γ is hyperparameter in focal loss. Note that, the focal loss is a widely-used loss for class imbalance issue [38,39]. To further improve the classification performance, we encourage high-density compactness of intra-class samples and low-density separation of inter-class samples for all domains via entropy minimization [21]:

$$\mathcal{L}_{en}(\theta_f, \theta_m, \theta_y) = -\frac{1}{n_t + n_s} \sum_{i=1}^{n_t+n_s} \hat{\mathbf{y}}_i^\top \log(\hat{\mathbf{y}}_i). \tag{4}$$

Based on the above, we summarize the overall classification loss $\mathcal{L}_c$ as follows:

$$\mathcal{L}_c(\theta_f, \theta_m, \theta_y) = \mathcal{L}_{fo}(\theta_f, \theta_m, \theta_y) + \eta \mathcal{L}_{en}(\theta_f, \theta_m, \theta_y), \tag{5}$$

where η is a hyperparameter to trade-off between the two losses.

Table 1. Statistics of the AS-OCT dataset.

Domain	Data	Country	Device	Training set			Test set		
				#Narrow	#Open	#Total	#Narrow	#Open	#Total
Source	AS-I	China	CASIA-I	3,006	6,024	9,030	790	1412	2,202
Target I	AS-II	China	CASIA-II	62	464	526	64	464	526
Target II	AS-III	Singapore	CASIA-I	416	1,406	1,822	418	1,406	1,824

3   Experiments

Dataset. In this paper, we conduct our experiments on one anterior segment optical coherence tomography (AS-OCT) dataset, provided by Zhongshan Ophthalmic Center. Such a dataset consists of a well-labeled source domain (**AS-I**) and two unlabeled target domains (**AS-II** and **AS-III**). The data from different domains are acquired from different OCT devices and/or different countries. The statistics of the dataset are shown in Table 1.

Compared methods. We compare our proposed M2DAN with one baseline (**Source-only**), several state-of-the-art unsupervised domain adaptation methods (**DSN** [3], **DANN** [8], **DMAN** [38] and **ToAlign** [35]), and one advanced multi-target domain adaptation methods for natural images (**MTDA** [11]). The baseline Source-only is trained only on the labeled source domain.

Implementation details. We implement our proposed method based on PyTorch [25]. For a fair comparison, we use res2net [9] as the feature extractor in all considered methods. (one can also use other DNN models, *e.g.,* ResNet [14] and MobileNetV2 [30]). For all compared methods, we keep the same hyperparameters as the original paper. Note that we conduct pair-wise domain adaptation for each target domain separately when implementing unsupervised domain adaptation methods. For M2DAN, both classifier and domain discriminator consist of three fully connected layers. In the training process, we use an SGD optimizer with a learning rate of 0.001 to train the network. For the trade-off parameters, we set $\lambda = 1.0$, $\eta = 0.1$ and $\alpha = 0.03$ through cross-validation. Following [17], we set $\gamma = 2.0$ for the focal loss. Following [6], we cut the images in half as the input of the network.

3.1   Comparisons with State-of-the-art Methods

We compare our M2DAN with several state-of-the-art methods in terms of two metrics, *i.e.,* accuracy and AUC [20]. From Table 2, all domain adaptation methods perform better than Source-only, which verifies the contribution of unsupervised domain adaptation. Moreover, our proposed M2DAN outperforms all pairwise unsupervised domain adaptation methods (*i.e.,* DSN, DANN, DMAN and DANN+ToAlign). The result indicates that those pair-wise domain adaptation methods may fail to alleviate the discrepancies among multiple domains since

Table 2. Comparisons of six methods in accuracy and AUC on two target domains.

Method	AS-II		AS-III		Mean Acc.	Mean AUC
	Acc.	AUC	Acc.	AUC		
Source-only	0.638	0.834	0.737	0.911	0.688	0.872
DANN [8]	0.723	0.866	0.836	0.912	0.780	0.889
DSN [3]	0.762	0.888	0.848	0.915	0.805	0.901
DMAN [38]	0.786	0.906	0.834	0.922	0.810	0.914
DANN+ToAlign [35]	0.842	0.685	0.688	0.607	0.765	0.646
MTDA [11]	0.667	0.791	0.735	0.806	0.701	0.799
M2DAN (ours)	**0.856**	**0.914**	**0.869**	**0.928**	**0.862**	**0.921**

Table 3. Effect of the filter size in the multi-scale module. The variant M2DAN-Sk represents the convolutional layers in all three branches of the multi-scale module use the same filter size k, where k=1, 3, 5.

Method	AS II		AS III		Mean Acc.	Mean AUC
	Acc.	AUC	Acc.	AUC		
M2DAN-S1	0.737	0.847	0.807	0.909	0.772	0.878
M2DAN-S3	0.756	0.913	0.748	0.916	0.752	0.914
M2DAN-S5	0.757	0.902	0.792	0.921	0.775	0.914
M2DAN	**0.856**	**0.914**	**0.869**	**0.928**	**0.862**	**0.921**

they focus on pair-wise adaptation and cannot capture correlation among domains effectively. In addition, M2DAN also outperforms MTDA in terms of both metrics, which demonstrates the superiority of our proposed method in handling multi-target domain adaptation for angle closure classification. In M2DAN, the multi-scale scheme helps to extract multi-scale domain-invariant features of AS-OCT images for angle closure classification. Note that the performance of MTDA is worse than pair-wise domain adaptation methods. Such poor performance of MTDA results from the poor reconstruction which includes a lot of noise for fine-grained anterior chamber angle in AS-OCT images.

3.2   Ablation Studies

The Effectiveness of Multi-scale Module. To verify the effectiveness of the proposed multi-scale module, we compare our method with three variants, namely **M2DAN-S1**, **M2DAN-S3** and **M2DAN-S5**. The variant **M2DAN-Sk** uses the same filter size k in all three branches of convolutional layers in the multi-scale module. In this case, the feature maps in each variant are extracted at the same scale. From Table 3, M2DAN achieves better performance than all three variants in terms of two target domains. The results demonstrate the superiority of the proposed multi-scale module.

Ablation Studies on Difference Losses. To investigate the effect of all losses ($\mathcal{L}_{fo}$, $\mathcal{L}_d$ and $\mathcal{L}_{en}$), we evaluate the model optimized by different losses. From

Table 4. Ablation study for the losses (*i.e.*, $\mathcal{L}_{fo}$, $\mathcal{L}_d$ and $\mathcal{L}_{en}$). Note that $\mathcal{L}_{ce}$ denotes the cross-entropy loss for angle closure classification.

Backbone	$\mathcal{L}_{ce}$	$\mathcal{L}_{fo}$	$\mathcal{L}_d$	$\mathcal{L}_{en}$	AS II		AS III		Mean Acc.	Mean AUC
					Acc.	AUC	Acc.	AUC		
	✓	✓			0.784	0.826	0.780	0.903	0.782	0.865
	✓		✓		0.828	0.843	0.814	0.894	0.821	0.868
	✓		✓	✓	0.856	0.876	0.841	0.916	0.848	0.896
	✓		✓	✓	**0.856**	**0.914**	**0.869**	**0.928**	**0.862**	**0.921**

Table 5. Influence of the trade-off parameter α on AUC performance of our method. The value of α is selected among [0.0003, 0.003, 0.03, 0.3], while fixing other parameters.

α	AS-II	AS-III	Mean AUC
$3e{-}04$	0.828	0.910	0.869
$3e{-}03$	0.909	0.892	0.901
$3e{-}02$	**0.914**	**0.928**	**0.921**
$3e{-}01$	0.813	0.843	0.828

Table 6. Influence of the trade-off parameter η on AUC performance of our method. The value of η is selected among [0.001, 0.01, 0.1, 1], while fixing other parameters.

η	AS-II	AS-III	Mean AUC
$1e{-}03$	0.791	0.871	0.831
$1e{-}02$	0.825	0.876	0.851
$1e{-}01$	**0.914**	**0.928**	**0.921**
1	0.884	0.922	0.903

Table 4, our method with $\mathcal{L}_{fo}$ performs better than that with $\mathcal{L}_{ce}$, verifying that the focal loss helps to handle the class-imbalanced issue. When introducing $\mathcal{L}_d$, the performance improves a lot, which indicates that such a loss succeeds in alleviating domain discrepancies among domains. By combining all the losses, we obtain the best result. Such a result demonstrates that encouraging high-density compactness of intra-class samples and low-density separation of inter-class samples further facilitates the classification of angle closure.

3.3   Influence of Hyper-parameter

In this section, we investigate the impact of the hyper-parameters α, η and λ. We evaluate one parameter a time while fixing other parameters. As shown in Tables 5, 6 and 7, our method achieves the best performance when setting $\alpha = 0.03$, $\eta = 0.1$ and $\lambda = 1$. To some extent, our method is non-sensitive to hyper-parameters. Moreover, it is crucial to set a reasonable classification loss weight which helps to classify angle closure effectively.

Table 7. Influence of the trade-off parameter λ on AUC performance of our method. The value of λ is selected among [0.001, 0.01, 0.1, 1], while fixing other parameters.

λ	AS-II	AS-III	Mean AUC
$1e-03$	0.663	0.671	0.667
$1e-02$	0.709	0.647	0.678
$1e-01$	0.659	0.815	0.737
1	**0.914**	**0.928**	**0.921**

4   Conclusion

In this paper, we have proposed a novel Multi-scale Multi-target Domain Adversarial Network (M2DAN) for angle closure classification. M2DAN aims to transfer a deep model learned on one labeled source domain to multiple unlabeled target domains. To be specific, we devise a multi-scale module to extract features regarding both local and global information. By performing multi-domain adversarial learning at different scales, M2DAN is able to extract domain-invariant features and effectively classify angle closure in multiple target domains. Extensive experiments demonstrate the effectiveness of our proposed method.

Acknowledgments

References

1. Azzeh, J., Zahran, B., Alqadi, Z.: Salt and pepper noise: Effects and removal. JOIV: International Journal on Informatics Visualization **2**(4), 252–256 (2018)
2. Benaim, S., Wolf, L.: One-sided unsupervised domain mapping. In: Advances in neural information processing systems. pp. 752–762 (2017)
3. Bousmalis, K., Trigeorgis, G., et al.: Domain separation networks. In: Advances in neural information processing systems. pp. 343–351 (2016)
4. Dubbelman, M., Van der Heijde, G., et al.: Change in shape of the aging human crystalline lens with accommodation. Vision research **45**(1), 117–132 (2005)
5. Fu, H., Li, F., Sun, X., et al.: Age challenge: Angle closure glaucoma evaluation in anterior segment optical coherence tomography. Medical Image Analysis **66**, 101798 (2020)
6. Fu, H., Xu, Y., Lin, S., et al.: Segmentation and quantification for angle-closure glaucoma assessment in anterior segment oct. IEEE transactions on medical imaging **36**(9), 1930–1938 (2017)
7. Fu, H., Xu, Y., Lin, S., et al.: Multi-context deep network for angle-closure glaucoma screening in anterior segment oct. In: International Conference on Medical Image Computing and Computer-Assisted Intervention. pp. 356–363. Springer (2018)

8. Ganin, Y., Lempitsky, V.: Unsupervised domain adaptation by backpropagation. arXiv preprint arXiv:1409.7495 (2014)
9. Gao, S., Cheng, M.M., Zhao, K., et al.: Res2net: A new multi-scale backbone architecture. IEEE transactions on pattern analysis and machine intelligence (2019)
10. Ghafoorian, M., Mehrtash, A., Kapur, T., et al.: Transfer learning for domain adaptation in mri: Application in brain lesion segmentation. In: International conference on medical image computing and computer-assisted intervention. pp. 516–524. Springer (2017)
11. Gholami, B., Sahu, P., Rudovic, O., et al.: Unsupervised multi-target domain adaptation: An information theoretic approach. IEEE Transactions on Image Processing **29**, 3993–4002 (2020)
12. Hao, H., Zhao, Y., Yan, Q., et al.: Angle-closure assessment in anterior segment oct images via deep learning. Medical Image Analysis **69**, 101956 (2021)
13. Hao, J., Li, F., Hao, H., et al.: Hybrid variation-aware network for angle-closure assessment in as-oct. IEEE Transactions on Medical Imaging (2021)
14. He, K., Zhang, X., Ren, S., Sun, J.: Deep residual learning for image recognition. In: Proceedings of the IEEE conference on computer vision and pattern recognition. pp. 770–778 (2016)
15. Leung, C.K., Weinreb, R.: Anterior chamber angle imaging with optical coherence tomography. Eye **25**(3), 261–267 (2011)
16. Lin, H., Zhang, Y., Qiu, Z., et al.: Prototype-guided continual adaptation for class-incremental unsupervised domain adaptation. In: European Conference on Computer Vision (2022)
17. Lin, T.Y., Goyal, P., Girshick, R., et al.: Focal loss for dense object detection. In: Proceedings of the IEEE international conference on computer vision. pp. 2980–2988 (2017)
18. Litjens, G., Kooi, T., Bejnordi, B.E., et al.: A survey on deep learning in medical image analysis. Medical image analysis **42**, 60–88 (2017)
19. Liu, Y., Du, X.: Duda: Deep unsupervised domain adaptation learning for multi-sequence cardiac mr image segmentation. In: Chinese Conference on Pattern Recognition and Computer Vision (PRCV). pp. 503–515. Springer (2020)
20. Lobo, J.M., Jiménez-Valverde, A., Real, R.: Auc: a misleading measure of the performance of predictive distribution models. Global ecology and Biogeography **17**(2), 145–151 (2008)
21. Mangin, J.F.: Entropy minimization for automatic correction of intensity nonuniformity. In: Proceedings IEEE Workshop on Mathematical Methods in Biomedical Image Analysis. MMBIA-2000 (Cat. No. PR00737). pp. 162–169. IEEE (2000)
22. Niu, S., Wu, J., Zhang, Y., et al.: Efficient test-time model adaptation without forgetting. In: International Conference on Machine Learning (2022)
23. Niwas, S.I., Lin, W., Bai, X., et al.: Automated anterior segment oct image analysis for angle closure glaucoma mechanisms classification. Computer methods and programs in biomedicine **130**, 65–75 (2016)
24. Nongpiur, M.E., Haaland, B.A., Friedman, D.S., et al.: Classification algorithms based on anterior segment optical coherence tomography measurements for detection of angle closure. Ophthalmology **120**(1), 48–54 (2013)
25. Paszke, A., Gross, S., Massa, F., et al.: Pytorch: An imperative style, high-performance deep learning library. In: Advances in Neural Information Processing Systems. pp. 8024–8035 (2019)
26. Peng, X., Huang, Z., Sun, X., Saenko, K.: Domain agnostic learning with disentangled representations. arXiv preprint arXiv:1904.12347 (2019)

27. Qiu, Z., Zhang, Y., Lin, H., et al.: Source-free domain adaptation via avatar prototype generation and adaptation. In: International Joint Conference on Artificial Intelligence (2021)
28. Quigley, H.A., Broman, A.T.: The number of people with glaucoma worldwide in 2010 and 2020. British journal of ophthalmology **90**(3), 262–267 (2006)
29. Ren, J., Hacihaliloglu, I., Singer, E.A., et al.: Adversarial domain adaptation for classification of prostate histopathology whole-slide images. In: International Conference on Medical Image Computing and Computer-Assisted Intervention. pp. 201–209. Springer (2018)
30. Sandler, M., Howard, A., Zhu, M., et al.: Mobilenetv2: Inverted residuals and linear bottlenecks. In: Proceedings of the IEEE conference on computer vision and pattern recognition. pp. 4510–4520 (2018)
31. Thylefors, B., Negrel, A., Pararajasegaram, R., Dadzie, K.: Global data on blindness. Bulletin of the world health organization **73**(1), 115 (1995)
32. Tzeng, E., Hoffman, J., Saenko, K., Darrell, T.: Adversarial discriminative domain adaptation. In: Proceedings of the IEEE Conference on Computer Vision and Pattern Recognition. pp. 7167–7176 (2017)
33. Tzeng, E., Hoffman, J., Zhang, N., et al.: Deep domain confusion: Maximizing for domain invariance. arXiv preprint arXiv:1412.3474 (2014)
34. Wang, S., Zhang, L.: Lstn: Latent subspace transfer network for unsupervised domain adaptation. In: Chinese Conference on Pattern Recognition and Computer Vision (PRCV). pp. 273–284. Springer (2018)
35. Wei, G., Lan, C., Zeng, W., Chen, Z.: Toalign: Task-oriented alignment for unsupervised domain adaptation. In: NeurIPS (2021)
36. Yang, J., Dvornek, N.C., Zhang, F., et al.: Domain-agnostic learning with anatomy-consistent embedding for cross-modality liver segmentation. In: Proceedings of the IEEE International Conference on Computer Vision Workshops. pp. 0–0 (2019)
37. Zhang, X., Luo, H., Fan, X., et al.: Alignedreid: Surpassing human-level performance in person re-identification. arXiv preprint arXiv:1711.08184 (2017)
38. Zhang, Y., Chen, H., Wei, Y., et al.: From whole slide imaging to microscopy: Deep microscopy adaptation network for histopathology cancer image classification. In: International Conference on Medical Image Computing and Computer-Assisted Intervention. pp. 360–368. Springer (2019)
39. Zhang, Y., Kang, B., Hooi, B., et al.: Deep long-tailed learning: A survey. arXiv preprint arXiv:2110.04596 (2021)
40. Zhang, Y., Wei, Y., Wu, Q., et al.: Collaborative unsupervised domain adaptation for medical image diagnosis. IEEE Transactions on Image Processing **29**, 7834–7844 (2020)
41. Zhou, J., Wu, F., Sun, Y., et al.: Adversarial domain alignment feature similarity enhancement learning for unsupervised domain adaptation. In: Chinese Conference on Pattern Recognition and Computer Vision (PRCV). pp. 259–271. Springer (2019)